

# Lung Mesh Generation to Simulate Breathing Motion with a Finite Element Method.

Pierre-Frédéric Villard, Michaël Beuve, Behzad Shariat, Vincent Baudet and Fabrice Jaillet  
pierre-frederic.villard@liris.univ-lyon1.fr  
LIRIS, bat Nautibus, 8 bd Niels Bohr, 69622 Villeurbanne CEDEX, FRANCE

## Abstract

*Numerical modelling of lung behaviour during the respiration cycle is a difficult challenge due to its complex geometry and surrounding environment constraints.*

*This paper presents an approach to simulate a patient's lung motion during inhaling and exhaling based on a continuous media mechanics model and solved with a finite element method.*

*One of the key problems is an adequate lung mesh generation, which is specifically developed in this paper.*

**keywords :** lung mechanics, finite elements, mesh, behaviour and geometric modelling

## 1 Introduction

Currently, new technologies make the radiotherapy more effective. Among these evolutions, let us quote Intensity-Modulated Radiation Therapy (or IMRT), which gives a better treatment conformation to tumour shape. Hadrontherapy permits a great accuracy and a great efficiency due to the energy deposit of light ions inside the tumours, delivering high radiation doses in deep tumours with a higher radiobiological effect. These new technologies require a more elaborated ballistics control compelling an increased control of organ motions not only during the treatment planning but as well while performing the treatment.

Different approaches exist to take into account lung motion during the treatment: gating and tracking. Gating could be either a breathing gating, which allows to hold lung into a well determined inflating volume, thus finally permitting a static treatment; or a beam gating, which treats only tumours when at a known position. Tracking is a method based on a treatment that conforms to the tumours movements in their environment, allowing the patient to breath normally. All of these techniques and particularly the last one, require a good knowledge of the influence of

tumour displacements and deformations on the quality of the treatment.

In this paper, after a short survey of recent works on lung motion modelling, we present our approach to represent a lung and its environment using the continuum media mechanics formalism. This necessitates the meshing of treated volumes under consideration. Using a finite element technique, we can estimate organs deformation and displacement by the application of the environmental constraints to the mesh. The following sections summarise the finite element technique and present in detail our mesh generation approach.

## 2 Recent survey

A recent work studies experimentally the effect of the thoracic motion on different organs with the use of a 4D CT scan [11]. In this context, this technology becomes useful due to recent improvement of CT scan technology and acquisition time and to a significant reduction of motion artifacts. To obtain temporal information, data are acquired in axial cine-scan mode and they are indexed with abdomen motion for the duration of a set of patient's respiratory cycles. Several images per scanner-slice position are used for reconstruction, each representing a different point in time within the respiratory cycle. Images from different scanner-slice positions are then sorted into several spatio-temporal coherent CT volumes permitting to study the motion of lung tumours based on manual segmentation of 4D CT scan data [10].

In [4], breath holding techniques were used to acquire different CT scans at different breathing stages. The authors developed non-rigid registration tools to evaluate the reproducibility of the breath control device for each patient, and to extract motion information for subsequent dosimetric and modelling studies. Given two images, the method consists in estimating the displacement vector field allowing to determine for each point in the first image the corresponding points in the second one. The results show that, by comparing vector fields between several acquisitions taken at

the same initial and final breath hold level, it is possible to quantify organs displacement in order to adapt margins for the treatment planning.

In a previous work [2] we presented our contribution to the simulation of lung behaviour with 3D dynamic deformable models in order to obtain models of tumour displacement. These models were customised to the patient's anatomical and physiological parameters. The advantages of such simulation techniques are various. (1) It avoids to introduce an interpolation process for filling the temporal gaps of 3D CT scan sequences. Each breathing step can be computed by a simulation based on a curve of respiratory cycle. (2) Contouring of tumour by medical doctors only has to be realised once. Indeed the models predict tumour movement and deformation over the respiration cycle. (3) These models moreover provide a convenient tool to study the behaviour of various kind of tumours. Therapeutic treatment can be planified with different positions, forms and sizes of tumour. Safety margin optimisation or other strategies can be developed and improved without the necessity of multiplying acquisition on real patients. (4) These methods are complementary to the one exposed in [4]. A comparison between the two teams is being performed.

Actually, two works are carried out: one based on a mass-spring system and the other based on finite elements techniques. The latter is only applicable for perpendicular displacements around the rib cage and perpendicular to the surface. Indeed the application of external forces induces unrealistic peaks of displacements. In this paper, we will especially focus on the finite element method.

### 3 Link between continuum media mechanics and lung mechanics

Let us introduce some notions about continuum media mechanics. The associated laws are commonly used to model solids in mechanical design. However, in this study, our goal is to link these laws to a bio-material: the lung. Indeed, a detailed modelling of lung structures at atomic and molecular scale are not required here. Hence, the assumption of continuum media can be applied to macroscopic level definition of organs.

In a global approach and as a first approximation, a homogeneous constant of elasticity - the Young modulus - can be used to parameterise the lung inflation. This is rather easy way to link with patient's data [2]. In the future, heterogeneity of the Young modulus and other mechanical properties will be taken into account. At the first step, we have used a linear elasticity, but our model can be easily extended to non linear behaviour with a Young modulus and a work hardening rate to simulate material solidification during defor-

mation. Various estimations of Poisson's ratio of the lung can be found in [9, 7, 6]. Nevertheless, it has been shown that the variation of the Poisson's ratio does not significantly change the results.

After this "rheological" introduction to biomaterial parametrisation, let us now focus on the type of analysis to be proceeded. During normal breathing, constraints are applied on the pleura steadily and progressively. Lung is wrapped in the pleura and we can consider its motion as a sequence of positions controlled only by its surface. Finally, we can assume a quasi static approach, *i.e.* the effects of inertia are neglected. Using an elastic model with a static analysis and knowing the external displacements, the absolute value of the Young modulus will no longer be necessary.

Commonly, lung volume can increase by a factor of two during a respiration cycle. The displacements are too large to assume that geometry changes will not influence the mechanical behaviour. Large deformations have then to be considered. Therefore, we employ the algorithm presented in [12] to take them into account. This algorithm uses an Eulerian formulation with a geometry reactualisation and an incremental resolution.

Let's consider the Fig.1 to illustrate our approach:

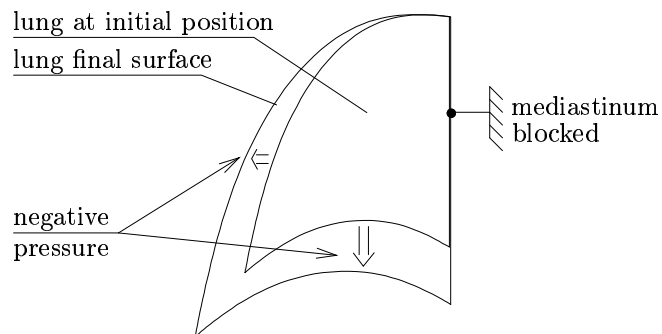


Figure 1. Constraints application scheme

In this figure, lung is presented at its initial and final states. The goal is to define the surrounding spatial constraints limit conditions. To respect them, a uniform negative pressure is applied around the lung at its first state to simulate pleural elastic recoil pressure. The motion stops when lung surface matches with its final state surface but nevertheless including possible skin slide (contact condition). We have also considered that mediastinum is fixed achieving then the whole necessary boundary conditions.

To solve this contact condition we use [13]. The algorithm of unilateral contact treatment consists in adding special equations on moving parts that are potentially in contact with a blocked surface. These equations are constituted by kinematic conditions of non penetration. The geometry is updated at each iteration.

The final strategy will be to monitor the lung infla-

tion by two parameters reproducing the diaphragmatic and rib-cage actions. We can consider thorax motion capture, acquired by a chest band or by video sensors. A diaphragm motion function can be determined by a dynamic 3D reconstruction with the respiration curve measured with a spirometer like in [5].

The complex geometry of lung and its anisotropic behaviour do not allow to develop an analytic solution for the set of equations introduced by this formalism. Therefore, we used the finite element method to approximate the lung displacements and deformations.

## 4 Lung motion simulation

### 4.1 Finite Element Method notions

The finite element method [14] is employed in many scientific fields to solve partial derivative equations. It consists in approximating the solution by a simpler expression in order to transform these continuous equations into a matrix representation.

For this, local partial derivative equations are firstly transformed into a global variational formulation. The variational formulation of a problem, starting from partial derivative equations, can be obtained by multiplying the latter by "test functions", integrating over the whole domain and using Green formula to obtain terms that concern only a boundary part of the domain. The test functions are "sufficiently" regular functions, which ponderate the global integral. In solid mechanics, the variational formulation obtained is identical to the Principle of Virtual Work.

In our case, we assume a structure  $\Omega$  with the volume density  $\rho$ , subject to bulk forces  $f$ , with imposed displacements  $U^D$  on the boundary  $\Gamma^D$  and imposed forces  $g^N$  on the boundary  $\Gamma^N$ . The local equations of static equilibrium on this structure can be written as:

$$\begin{cases} \operatorname{div}(\sigma) + \rho \cdot f = 0 & \text{in } \Omega \\ U = U^D & \text{in } \Gamma^D \\ f = g^N & \text{in } \Gamma^N \end{cases} \quad (1)$$

where  $U$  is the displacement tensor and  $\sigma$  is the stress tensor. The constitutive equation, which represents the material properties, has to be taken into account. It gives a relationship between the deformation  $\epsilon$  and  $\sigma$ . In the elastic case we have:  $\sigma = K \cdot \epsilon$ , where  $K$  is the elasticity matrix. The variational formulation gives then the same expression as the one given by the Principle of Virtual Work.

The displacement field  $u$ , satisfying  $\forall v \in \Gamma^D$  can be obtained by:

$$\underbrace{\int_{\Omega} \sigma(u) \cdot \epsilon(v) d\Omega}_{A(u,v)} = \underbrace{\int_{\Omega} \rho f \cdot v d\Omega + \int_{\Gamma^N} g^N \cdot v d\Gamma}_{B(v)} \quad (2)$$

Equation 2 takes into account the mass conservation, which is necessary in the case of large displacements. This equation can be resumed to  $A(u, v) = B(v), \forall v \in \Gamma^D$

To find an approximated solution, we discretise the displacement field. That is to say, we choose to calculate the displacement field at a set of  $N$  discrete points in the solid (called 'nodes' in finite element terminology). The structure is then cut out into "pieces" called elements. Node coordinates and connectivities constitute a mesh. One element of the mesh is defined by its geometry: triangle, quadrangle, tetrahedron, ... We will denote the coordinates of these special points by  $X^\alpha$ , where the superscript  $\alpha$  ranges from 1 to  $N$ . The unknown displacement vector at each nodal point will be denoted by  $(U_x^\alpha, U_y^\alpha, U_z^\alpha)$ . The displacement field at an arbitrary point within the solid will be specified by interpolating between nodal values in some convenient way  $U_i(X) = \sum_{\alpha=1}^N w^\alpha(X) U_i^\alpha$ . Here,  $X$  denotes the coordinates of an arbitrary point in the solid. The shape functions  $w^\alpha$  are depending on position only, which must have the following property such that

$$w^\alpha(X^\beta) = \begin{cases} 1 & \text{if } \alpha = \beta \\ 0 & \text{if } \alpha \neq \beta \end{cases} \quad (3)$$

We can obviously interpolate the virtual displacement field in exactly the same way. We can therefore re-write the variational formulation, substituting the interpolated fields in equation 2. Then, we obtain an equation system by merging the contributions coming from each element that contains the corresponding node. This is a system of  $N$  equations for the  $N$  nodal displacements. If  $A(u, v)$  is a linear application in  $u$ , the terms  $A(u_i, v_i)$  give a  $u_i$  linear system. If  $A(u, v)$  is not linear in  $u$ , the resolution is more complex. Despite of this, numerical methods could bring it back into a succession of linear problems.

Due to the continuity of the matter, the convergence rate directly depends on mesh accuracy. Moreover, for better accuracy and efficiency reasons, hexahedral elements are preferred to tetrahedral element [3]. The shape functions for a hexahedral element with eight nodes are:

$$\begin{aligned} w^1 &= 1/8(1-x)(1-y)(1-z) & w^5 &= 1/8(1-x)(1-y)(1+z) \\ w^2 &= 1/8(1+x)(1-y)(1-z) & w^6 &= 1/8(1+x)(1-y)(1+z) \\ w^3 &= 1/8(1+x)(1+y)(1-z) & w^7 &= 1/8(1+x)(1+y)(1+z) \\ w^4 &= 1/8(1-x)(1+y)(1-z) & w^8 &= 1/8(1-x)(1+y)(1+z) \end{aligned}$$

In the next step, the numerical simulation was carried out with the code-aster [1] finite element software.

### 4.2 mesh improvement

In [2], we have simply verified whether the numerical method presented above could converge to plausible results. We have obtained a hexahedral mesh from

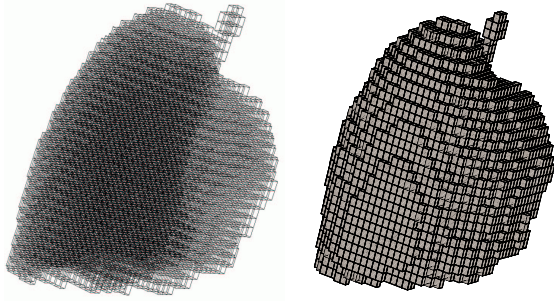


**Figure 2. hexahedral mesh (a.), quadrangle mesh (b.)**

segmented CT scan data, where each hexahedron corresponds to a CT scan voxel (Fig.2.a). External surface is then given by a quadrangular mesh (Fig.2.b).

Although our previous method converges while applying displacements in the direction of the surface gradient, it generates solutions not consistent with the reality if we apply a uniform pressure. Figure 3 shows the results of this simulation. The problem arises from stress-concentration artifact due to the sharp edges in cubes.

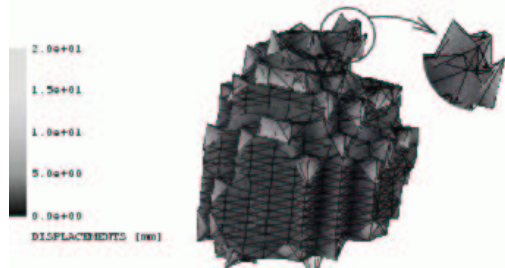


**Figure 3. geometry after applying a uniform pressure simulation**

This work aims at combining accuracy on the boundary surface and hexahedral mesh. Accuracy on the surface comes from a smooth external mesh. Hexahedral bulk mesh is convenient because it directly comes from CT scan and provides direct information on electronic density and probably for heterogeneity. Moreover, as mentioned before, hexahedral elements are preferred to tetrahedral element for finite element studies [3].

Motivated by a smoothness idea we used the marching cube (MC) algorithm presented in [8]. The virtual cube vertices are defined by the centres of eight CT scan voxels. For each of them, the information about material is obtained directly from the intensity of the 3D segmented images. If a vertex has a different material information from its neighbouring vertices, a boundary surface should exist between it and the others in order to separate different materi-

als. There are 256 different combinations of material informations that cube vertices could define. These combinations can be reduced to 15 situations with the classification of similar cases. The surface generation process is extremely fast due to the direct triangulation from the look-up-table properties of the marching cube routine. As shown in Fig.4.a, the surface model created by the MC algorithm has smoother curvatures than on the previous Fig.2.b. To fill this surface mesh with 3D elements, we build a 3D mesh with a traditional delaunay method (Fig.4.b.)

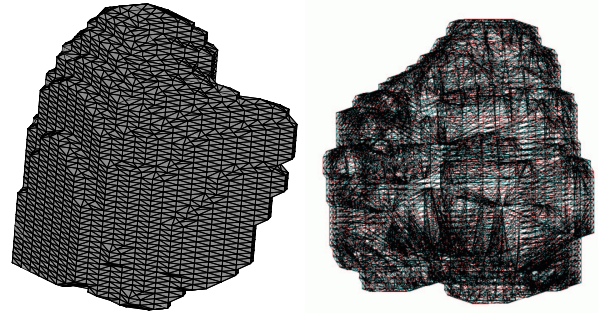


**Figure 4. triangle mesh issue from MC (a.), 3D Delaunay mesh (b.)**

Fig.5 shows the results of the contact method presented in section 3. From the initial state Fig.5.a, we apply a uniform pressure and a contact condition to the final state Fig.5.b. Smoothed edges obtained by the MC algorithm allows to compute contact with a uniform pressure. The results of the lung inflation simulation obtained with our method (Fig.5.c) fits well with lung models issued from CT scan voxel.

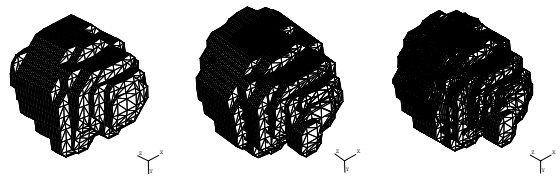


**Figure 5. lung at initial state (a.), lung at final state: from CT scan date (b.) and from the simulation (c.)**

A 3D mesh is necessary for our study and the one obtained with the Delaunay method allows us to check the validity of our method. However, it does not give enough information for our final goal : we have to add the internal hexahedral elements at least for dosimetry computation. Therefore, cubes extracted from the CT scan are added to the previous mesh, to have both internal elements and a smooth surface. Fig.6.a shows a lung cut where we can see a skin composed of tri-

angles and the internal 3D mesh composed of hexaedra. Fig.6.b shows a simulation of a uniform pressure applied to this geometry. From this numerical experiment, it appears some unexpected peaks, on the surface edges. This problem is due to the lack of elements.

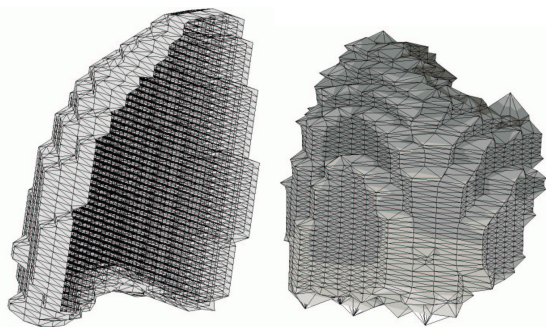


**Figure 6.** lung cut with 3D cubic mesh and a triangle surface mesh (a.), Uniform pressure simulation (b.)

Indeed, when we add a triangular mesh on an initial mesh composed of hexahedra, it appears some holes between elements. Fig.7, shows an illustration of this problem in 2D. The bold line, representing the triangular elements of the mesh, lets some unfilled space.

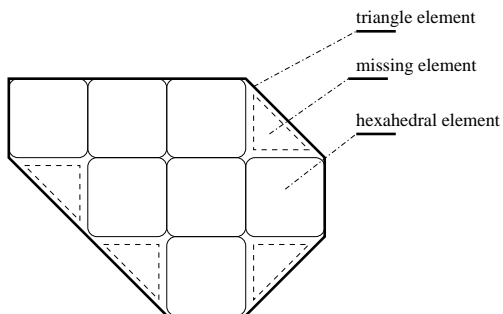


**Figure 7.** missing elements filling holes

In order to add the missing elements we propose an extension of the marching cube to provide tetrahedra for each of the 256 possible configurations of the method. For each list of triangles linked to a configuration we associate a list of tetrahedra too. In the classical marching cube, few configurations are studied because most of the arrangements are topologically equivalent. For example, there is no triangle when all eight nodes lie inside or outside the boundary surface. The Tab.1 shows examples of triangular patches. For each case, one can apply the same treatment to both configurations (where **B** is the complementary of **A**). In the case of internal hexahedra, two configurations have to be considered for each triangular patch. The Tab.1 shows three examples of triangular patches giving two different sets of configurations. The hexahedra arrangement depends on the direction of the normals

of triangular patches.

	configuration A	configuration B
case 1		
case 2		
case 3		

**Table 1.** 6 examples of configurations for the MC 3D extension

This 3D extension of the marching cube permits to directly extract triangles defining the external surface and tetrahedra defining a peripheral mesh. This accurate 3D mesh gathers the whole conditions to model external motion. Moreover, the bulk mesh is always constituted of hexahedra directly extracted from the CT scan. A lung mesh cut with our method is shown on Fig.8.a. Fig.8.b details the previous figure to focus on the three kinds of mesh element.

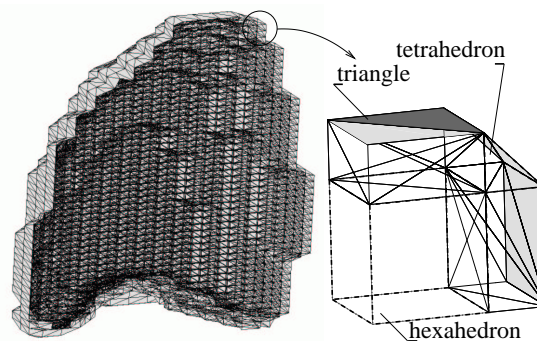


**Figure 8.** tetrahedral, triangle and hexahedral mesh (a.), detail (b.)

Finally, this geometry has been tested with a uniform pressure all around. Results are represented in Fig.9. The displacement field is totally smooth. There is no convergence problem due to mesh aberration.

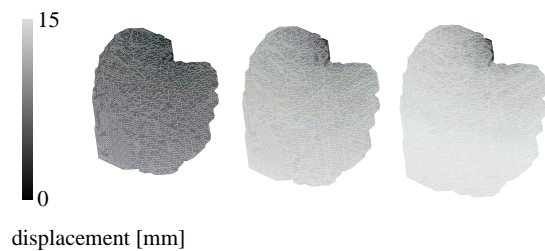


**Figure 9. three steps of a uniform inflating**

## 5 Conclusion

In this work, we have solved the convergence problem that has been pointed out in our previous study, using a special mesh based on the marching cube algorithm. This special mesh has many advantages: it gives an accurate contour for the external surface and an accurate mesh of the external stratum. The internal meshes are directly extracted from CT scan and the hexahedra are well suited for non-linear analysis. Moreover, information for dosimetry (electronic density) is straightforward.

## 6 Future Work

Firstly, we will add heterogeneity into the lung mechanical properties. A protocol is under elaboration to perform compression tests (to measure elasticity) on various samples of the same lung tissue.

Actually, we are working on the reconstruction of CT scan slices obtained from the sampling of our model at various levels of inflation. Indeed, these simulated CT scan images are useful quantities for treatment planning.

To test the validity of our model a study will estimate the difference between the simulated CT scans obtained from our model and the data from real CT scans.

Finally, we will extract thorax displacements on body surface and diaphragm motion to have the final simulation controlled by two parameters. Two teams are working on these topics.

## 7 Acknowledgements

We thank all our partners: the Léon Bérard Centre and the ETOILE<sup>1</sup> project for their support.

## References

[1] Code Aster. <http://www.code-aster.org/>.

<sup>1</sup>E.T.O.I.L.E.: Espace de Traitement Oncologique par Ions Légers, <http://ETOILE.univ-lyon1.fr>

- [2] V. Baudet, P-F. Villard, F. Jaillet, M. Beuve, and B. Shariat. Towards accurate tumour tracking in lungs. *Mediviz, Conference on Information Visualization*, pages 338–343, 2003.
- [3] S.E. Benzley, E. Perry, K. Merkle, B. Clark, and G.D. Sjaardema. A comparison of all hexagonal and all tetrahedral finite element meshes for elastic and elasto-plastic analysis. *Proceedings, 4th annual international meshing roundtable*, pages 179–191, 1995.
- [4] V. Boldea and D. Sarrut. Lung deformation estimation with non-rigid registration for radiotherapy treatment. *Medical Image Computing and Computer-Assisted Intervention MICCAI*, 2878:770–777, 2003.
- [5] S. Craighero. *Etude de faisabilité d'acquisition IRM dynamique du diaphragme au cours du cycle respiratoire*. PhD thesis, Université J. Fourier, 2001.
- [6] SJ Lai-Fook. Lung parenchyma described as a prestressed compressible material. *J Biomech.*, 10(5-6):357–65, 1977.
- [7] RK. Lambert and TA. Wilson. A model for the elastic properties of the lung and their effect of expiratory flow. *J Appl Physiol.*, 34:34–48, 1973.
- [8] W.E. Lorensen and H.E. Cline. Marching cubes: a high resolution 3d surface reconstruction algorithm. *Computer Graphics*, 21:163–169, 1987.
- [9] M.R. Owen and M.A. Lewis. The mechanics of lung tissue under high-frequency ventilation. *SIAM Journal on Applied Mathematics*, 61(5):1731–1761, 2001.
- [10] E. Rietzel, G. Chen, D. Kaeli, and B. Salzberg. Characterizing tumour motion using 4d computer tomography. *CenSSIS Research and Industrial Collaboration Conference*, 2003.
- [11] E. Rietzel and T. Pan K. Doppke. 4d computer tomography for radiation therapy. *Med Phys.*, 6:1365, 2003.
- [12] J.C. Simo and C. Miehe. Associative coupled thermoplasticity at finite strains: formulation, numerical analysis and implementation. *Comp. Meth. Appl. Mech. Eng.*, 98:41–104, 1992.
- [13] N. Tardieu. Contact unilatéral par des conditions cinématiques. *Code-Aster, documentation Référence, [R5.03.50]*, 2001.
- [14] O. C. Zienkiewicz. *La Méthode des éléments finis*. McGraw Hill Montréal Paris, 1979. Traduction de la 3ème édition anglaise.